Journal of Applied Electrochemistry (2020) 50:1037–1043
https://doi.org/10.1007/s10800-020-01457-6

RESEARCH ARTICLE

Investigation of oxygen evolution reaction performance of silver doped $Ba_{0.5}Sr_{0.5}Co_{0.8}Fe_{0.2}O_{3-\delta}$ perovskite structure

Emre Yusuf Göl[1] · Ahmet Aytekin[1] · Ecem Ezgi Özkahraman[1] · Engin Karabudak[1]

Received: 27 January 2020 / Accepted: 13 July 2020 / Published online: 19 August 2020

Abstract

Studies on novel electrochemical catalyst synthesis for efficient oxygen evolution reaction (OER) attract the attention of researchers. In general, changing of synthesis method and the doping metal affect the electrochemical activities of BSCF. In this work, silver doped $Ba_{0.5}Sr_{0.5}Co_{0.8}Fe_{0.2}O_{3-\delta}$ (BSCF-Ag) perovskite structure is shown to be a better electrocatalyst for oxygen evolution reaction (OER) due to its lower overpotential and extended durability. BSCF structure was synthesized by the EDTA-citric acid method. Appropriate amount of $Ba(NO_3)_2$ and EDTA were dissolved 0.1 M NH_4OH solution. Nitrate salts of other metals were dissolved in distilled water, then mixed with prepared $Ba(NO_3)_2$ solution. The mixture was stirred at 70 °C until gelation occurred. The gelled samples obtained were baked in a drying oven at 250 °C for 24 h before being calcined at 1000 °C for 12 h. To achieve a current density of 10 mA cm^{-2}, BSCF-Ag has required an overpotential of 0.36 V, which is very low compared to BSCF. To determine the stability of BSCF-Ag, continuous chronopotentiometry tests were carried out for 5 h and at a constant current density of 10 mA cm^{-2}. BSCF-Ag was characterized by XRD, SEM, and XPS.

Graphic abstract

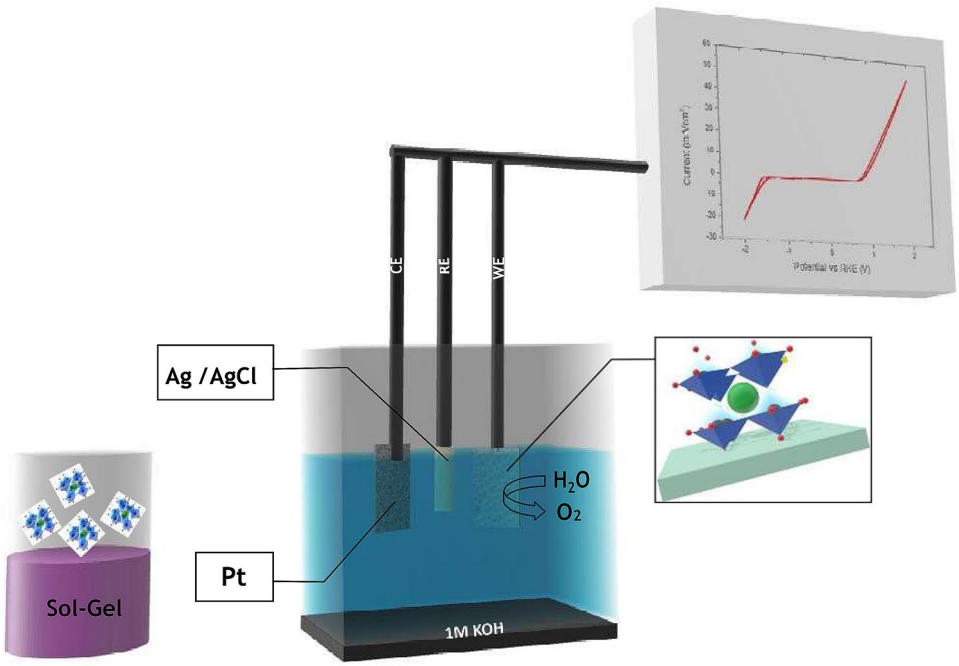

Keywords BSCF · Electrocatalyst · OER · LSV

Extended author information available on the last page of the article

1 Introduction

The environmental problems caused by the utilization of energy resources based on fossil fuels and the rapidly growing energy demand have gravitated the researchers towards efficient usage of sustainable energy resources such as, tidal, wind, and solar; and the improvement of storage and conversion technologies of these sources [1]. One of the critical solutions to these problems is the oxygen evolution reaction (OER), which is a significant method for many renewable energy devices [2–5]. In general, OER has intrinsically slow reaction kinetics because of its four-electron process, and as a result, OER has a substantial overpotential, compared to its thermodynamic potential [6]. To fulfill this potential requirement, rare metal-based catalysts, such as RuO_2 and IrO_2, are used as effective modern OER catalysts. At the same time, their high cost, low abundance, and low stability during long term operation impede their widespread applications [7].

Lately, a series of research concentrated around transition metal oxides exhibited particularly perovskite-type metal oxides with an stoichiometry of ABO_3 have promising OER action in basic media [8–11]. For instance, Suntivich et al. [9,12] indicated that BSCF perovskite has higher specific OER action than state-of-art IrO_2 electrocatalyst in basic media. Ba/Sr site, which is the A-site of perovskite structure, shows the most rapid oxygen transport kinetics and the cobalt rich B-site gives quicker oxygen exchange kinetic. To accomplish this progressively advantageous OER process, assignment of transition metal proportion at B-site could tune the e_g orbital filling (σ*-orbital occupation) [9]. Although the inherent action of BSCF is thought to be high, enormous molecule sizes obtained from the conventional bottom-up method [9] have restrained its functional applications to become widespread due to the low gravimetric mass movement. Another extreme issue for mechanical applications is the low durability of BSCF particles due to its surface amorphization under OER conditions [13].

The significant variations in the electrochemical activity of BSCF emerge from different synthesis and calcination methods, which directly affect the morphology and surface area of the structure. Furthermore, differences in electrode preparation give rise to inconsistencies about the OER activity of BSCF [14].

Silver, with its highest electrical conductivity, is the most abundant and cheapest noble metal [15–17]. In addition, silver nanoparticles show excellent stability in basic solutions [18]. An increase in electrochemical performance of catalysts that modified with silver, is expected [19]. Silver has high activity for oxygen reduction and evolution reactions [20,21], and this is likely to provide additional benefits to catalysts. Hence, the addition of silver is an ideal option to improve the electrochemical activity of BSCF.

In this study, we demonstrate the electrochemical catalytic performance and stability of silver doped-BSCF (BSCF-Ag) perovskite structure to observe whether there is an increase in these properties. There are lots of studies on solid oxide fuel cells related to silver doped-BSCF [22–31]. However, as far as we know, the effects of silver doping on BSCF for investigating OER activity have not been studied. Additionally, we compared the electrochemical activities of BSCF and BSCF-Ag. BSCF and BSCF-Ag were synthesized by using the sol–gel process. All perovskite structures were calcined under the same conditions. BSCF-Ag exhibited higher electrochemical performance than BSCF. Characterization of these perovskite structures was presented by using XRD, SEM, EDX, and XPS.

2 Experimental section

2.1 Synthesis of catalysts

Ethylenediaminetetraacetic acid (EDTA)-citrate method was used to synthesize the BSCF perovskite structures. The nitrate salts of Ba, Sr, Co, Fe, and Ag for the respective doped BSCF powder were dissolved in deionized water, stoichiometrically. $AgNO_3$ was added to achieve a silver ratio of 1% by weight in total. Complexing agents EDTA and citric acid were then added to the prepared solution, and the molar ratio was 1:1:2. To adjust pH to ~ 5, NH_4OH was added for complexation. The final solution was stirred for 24 h at 70 °C with 400 rpm until the gelation entirely occured. The obtained gelled samples were dried at 250 °C for an extra 24 h. Lastly, the collected material was calcinated at 1000 °C for 12 h to obtain the perovskite powder. Catalyst inks were prepared by using as-synthesized powders to use in the fabrication of the electrodes. A dispersion of 10 mg of synthesized perovskite powders and 10 mg carbon black were mixed with 100 µl of Nafion® and 1 ml of ethyl alcohol, and then the mixture was sonicated for 30 min to obtain catalyst inks.

2.2 Electrochemical measurements

Perovskite powders were coated on FTO glasses by using a drop-casting method. Firstly, FTO-coated glasses of 1×1 cm^2 were prepared. Then, the dispersed catalyst ink was coated onto the FTO surface with the loading of ~ 232 µg/cm^2. Coated glasses were annealed at 80 °C for 2 h. Cyclic voltammetry and linear sweep voltammetry measurements (LSV) were carried out by using the Metrohm PG-208 instrument. As reference and counter electrodes Ag/AgCl and Pt mesh were used, respectively. All the electrochemical measurements were performed in 1.0 M KOH solution. LSV measurements were done between 1 and 1,9 V vs. RHE.

Chronopotentiomemtric measurements were carried out at a constant current density of 10 mA cm^{-2} to determine the stability of catalysts.

3 Results and discussion

3.1 Materials structure & morphology

To decide the phases of BSCF and BSCF-Ag, we used X-ray diffraction (XRD) and Rietveld refinement analysis. In calcination temperatures below 700 °C, no characteristic diffraction peaks of Ag were found due to uniform dispersion over the surface of BSCF grains [28]. Figure 1 shows that a single crystallized perovskite structure was produced with the sol–gel method after a calcination process under air at 1000 °C for 12 h. Scherrer equation was used to determine the crystal size of BSCF-Ag and it was calculated as 32 nm. With the markers used, Fig. 1 shows the peaks arising from the introduction of silver into the perovskite structure. All diffraction peaks can be classified finely based on the cubic perovskite phase of BSCF. Ag and AgO phases were not observed. This indicates that silver is distributed uniformly in the spaces on the BSCF surface. No other peaks caused by impurities were detected. Rietveld refinement analysis results suggest that both BSCF and BSCF-Ag perovskite structures have cubic structure and similar lattice parameters. As shown in Table 1, Rietveld refinement results have a low-reliability factor, which indicates that the fitting of these results was reasonably good.

SEM images of perovskite structures are shown in Fig. 2. The porous size of BSCF is larger than BSCF-Ag, however, after modified Ag ion, this porous size has started to shrink. This show us that BSCF is successfully modified with Ag ion and Ag ion enters in holes which is found at BSCF in Fig. 2a. Besides, the surface is rougher at BSCF-Ag due to the aggregation of silver particles and decomposition of the perovskite surface, also it is seen that Modified-Ag particles are very clear in Fig. 2a. In the Table 2, EDX results of BSCF-Ag structure was shown. According to the EDX results, the amount of silver was in the desired ratio. To determine the specific surface area of BSCF and BSCF-Ag with BET, we used the nitrogen (N_2) sorption measurement method. Characteristic profiles of mesoporous structures were shown in both isotherms of perovskite materials. The specific surface area (S_{BET}) of BSCF and BSCF-Ag were measured 0.77 m^2g^{-1} and 1.85 m^2g^{-1}, respectively.

To decide the contents of perovskite structures X-ray photoelectron spectra (XPS) was used. XPS of BSCF and BSCF-Ag perovskite structures were shown in Fig. 3. Characteristic peaks for barium, cobalt, and oxygen are present intensely. At binding energies 775 and 792 eV, peaks of Ba $3p_{1/2}$ can be observed. Differentiating these peaks from Co peaks are difficult due to overlapping. The less intense peaks of Sr and Fe can be observed at 256 eV and 711 eV, respectively. Moreover, the peak of silver can be determined at 365 eV for the spectra of BSCF-Ag.

Table 1 Rietveld refined parameters and reliability factors of perovskites

Perovskites	Space group	Lattice parameter	X^2	R_p (%)	R_{wp} (%)
BSCF	*P*m-3 m	a = 3.992	1.978	3.10	5.44
BSCF-Ag	*P*m-3 m	a = 3.989	1.434	3.18	4.94

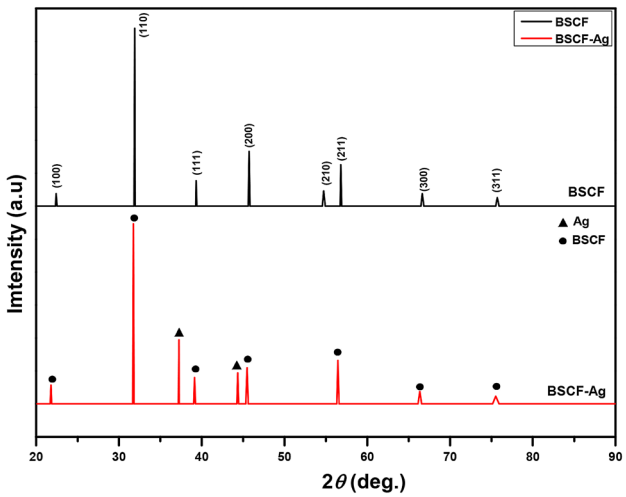

Fig. 1 XRD patterns of BSCF and BSCF-Ag powders

3.2 Oxygen evolution reaction performance

To measure linear sweep voltammograms (LSV) (Fig. 4a) of BSCF, and BSCF-Ag, we used a 3-electrode system in 1.0 mol L^{-1} KOH solution with a scan rate of 10 mV s^{-1} over the OER portion. The onset potential of state-of-art catalyst IrO_2 is 1.4 V vs. RHE [32]. BSCF-Ag exhibited an onset potential of 1.51 V vs. RHE, which is a good OER onset potential. Additionally, BSCF-Ag showed a better OER performance than pure BSCF.

An essential term for electrochemical solar fuel synthesis is overpotential (η), which specifies the necessary excessive potential to achieve the current density of 10 mA cm^{2-}.[33] Comparing the overpotentials of the as-synthesized catalysts at the specific current density of 10 mA cm^{2-}, the difference of theoretical reversible potential (1.23 V vs. RHE) and the significant potential to reach 10 mA cm^{2-} for OER is used to define overpotential in this study. The overpotential for BSCF-Ag to achieve 10 mA cm^{2-} current density is 0.44 V. This overpotential

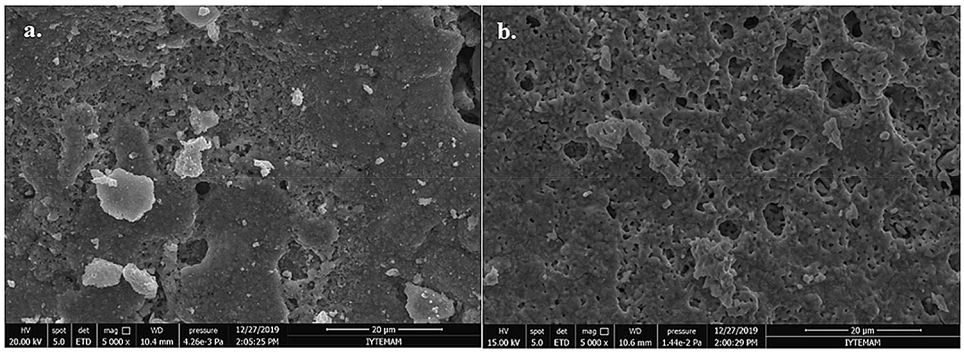

Fig. 2 SEM images of **a** BSCF-Ag and **b** BSCF perovskite oxides

Table 2 Chemical composition of BSCF-Ag perovskite structure resulting from the EDX analyzes

Element	Wt%
O	25.09
Fe	2.57
Co	14.06
Sr	18.07
Ag	0.96
Ba	39.25

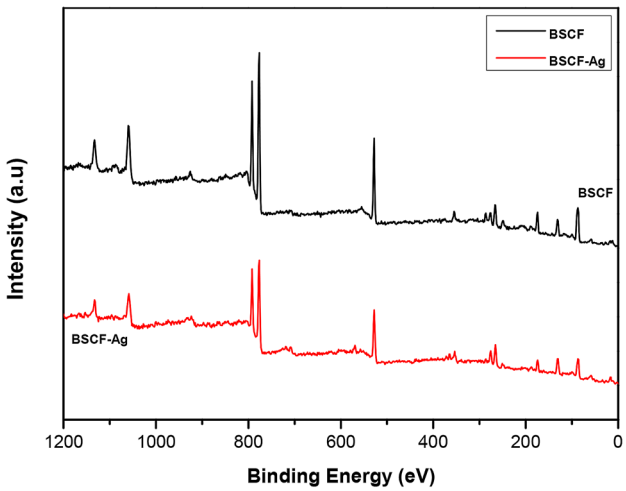

Fig. 3 X-ray photoelectron spectroscopy (XPS) spectra of BSCF and BSCF-Ag

is lower than the overpotential of BSCF but higher than the overpotential of IrO_2, which are 0.51 V and 0.32 V [33] respectively. In Table 3 we showed mass activity (MA) and specific activity (SA). The MA value of BSCF-Ag is 93.78 $Ag^{-1}{}_{cat}$ at a 550 mV overpotential (η. This value is higher than for BSCF (56.39 $Ag^{-1}{}_{cat}$). This value shows that BSCF- Ag has higher OER activity than pure BSCF. In Fig. 4b Tafel plots of BSCF and BSCF-Ag are demonstrated. The Tafel slope value for BSCF-Ag was less high than pure BSCF, which confirms that BSCF-Ag has faster kinetics than pure BSCF.

For practical applications, long term performance stability is an important factor. The performance stability of BSCF-Ag and BSCF were measured by using the chronopotentiometric (CP) test in a 1 M KOH solution. The CP tests were carried out in a 3-electrode cell. Catalyst ink was deposited on a FTO-coated glass with a dimension of 1 cm × 1 cm to reach a catalyst loading of 0.232 mg cm^{-2}. Figure 5 represents the long-term stabilities of BSCF powders for OER. Chronopotentiometric measurements were carried out at a constant current density of 10 mA cm^{-2} in 1.0 M KOH solution. Although both perovskite structures were very stable for 10 h, the BSCF-Ag structure has achieved this current density at a very low potential value, which also indicates its lower overpotential as an OER catalyst.

Lastly, we investigated the oxidation state of BSCF perovskite structures. For oxygen evolution reaction (OER), it is known that the greater amount of Co^{2+} leads to a shift towards higher binding energies [14,34]. Besides, it was shown that if Co^{2+} content of the perovskite structure has larger, its electrochemical activity as an OER catalyst is enhanced [35]. Because of overlapping between Co 2p and Ba 3d lines deciding the surface oxidation evolves into a tough challenge [36,37]. In Fig. 6, it can be seen that there is a shift towards higher binding energies for BSCF-Ag, which is the result of larger Co^{2+} content.

4 Conclusions

BSCF-Ag perovskite structure were synthesized to investigate its use as an OER electrocatalyst. We have found that silver doped BSCF perovskite structures show promising electrochemical performance for OER in basic media as a stable metal catalyst. Compared to undoped BSCF, BSCF-Ag perovskite structures showed better current density results in basic media for OER catalysis. Stability tests show that BSCF-Ag

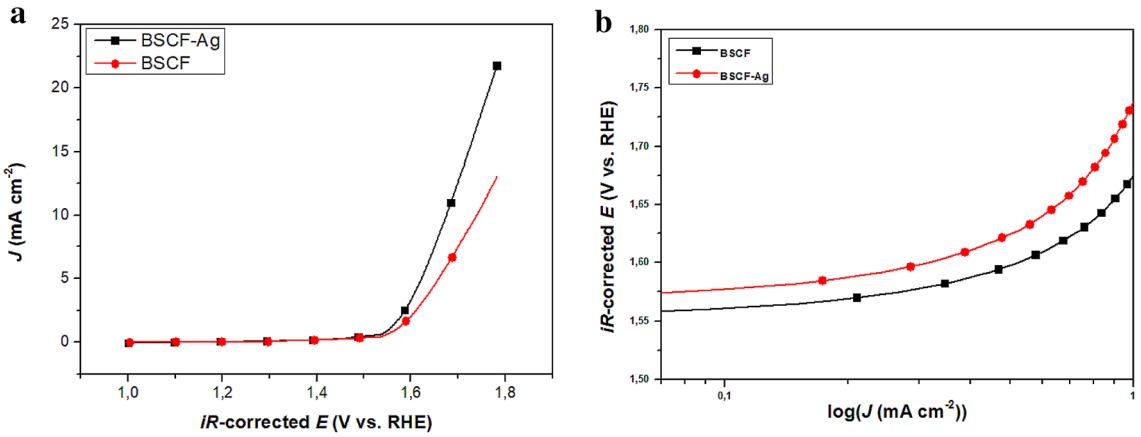

Fig. 4 LSVs for **a** BSCF and BSCF-Ag and **b** Tafel plots for perovskite structures between 0.1 and 0.5 mA cm^{-2}

Table 3 Summarization of OER performances of BSCF and BSCF-AG perovskite structures

Sample name	BET surface area ($m^2 \cdot g^{-1}$)	Overpotential at 10 $mA \cdot cm^{-2}$	Onset potential (V)	MA at 0.55 V ($A \cdot g^{-1}$)	SA at 0.55 V ($mA \cdot cm^{-2}$)	Tafel slope ($mV \cdot dec^{-1}$)
BSCF	0.77	0.51	1.54	56.29	7.3	281
BSCF-Ag	1.85	0.44	1.51	93.78	5.07	122

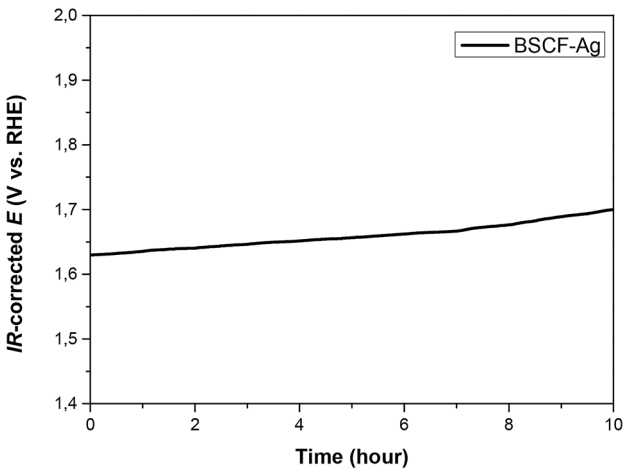

Fig. 5 Chronopotentiometric measurements of BSCF-Ag and BSCF maintaining a constant current density of 10 mA cm^{-2} in a 1 mol L^{-1} KOH solution

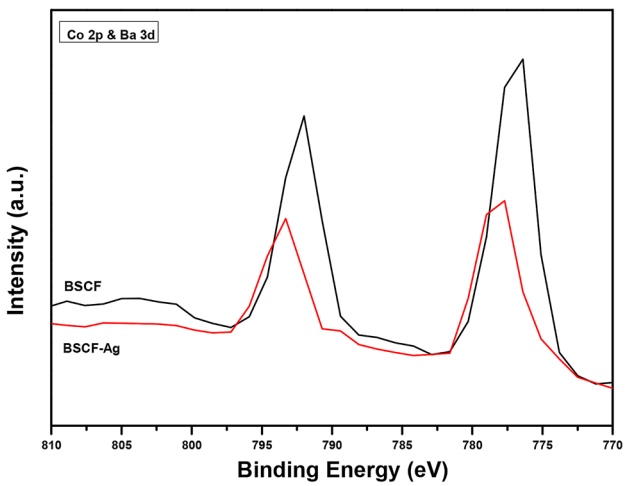

Fig. 6 XPS spectra of Co 2p and Ba 3d for BSCF-Ag and pure BSCF

powder to have slightly lower potential values after 10 h, which demonstrates their stability in 1.0 M KOH solution. XRD and SEM results showed that desired structures were synthesized successfully. Increment at the surface area of the perovskite structure was determined with BET analysis, which is consistent with SEM images. The Tafel slope of BSCF-Ag was lower than pure BSCF, which concludes that BSCF-Ag has faster OER kinetics. Because of its better conductivity and higher surface area, BSCF-Ag was shown to improve OER activity. The factor adding to the improved OER performance for BSCF-Ag in respect to BSCF has been debated, which are faster charge transfer rate and, larger electrochemically active surface area. Future studies should be carried out to determine the exact mechanism.

Acknowledgements Thanks to EAE Corporate and Siz+ Company and Mr. Yusuf Hikmet Kaya for their financial support.

References

1. Chu S, Majumdar A (2012) Opportunities and challenges for a sustainable energy future. Nature 488(7411):294–303. https://doi.org/10.1038/nature11475
2. Kim JS, Kim B, Kim H, Kang K (2018) Recent progress on multimetal oxide catalysts for the oxygen evolution reaction. Adv Energy Mater 8(11):1702774. https://doi.org/10.1002/aenm.201702774
3. Li G, Chuang P-YA (2018) Identifying the forefront of electrocatalytic oxygen evolution reaction: electronic double layer. Appl Catal B 239:425–432. https://doi.org/10.1016/j.apcatb.2018.08.037
4. Muthurasu A, Maruthapandian V, Kim HY (2019) Metal-organic framework derived Co_3O_4/MoS_2 heterostructure for efficient bifunctional electrocatalysts for oxygen evolution reaction and hydrogen evolution reaction. Appl Catal B 248:202–210. https://doi.org/10.1016/j.apcatb.2019.02.014
5. Xu X, Wang W, Zhou W, Shao Z (2018) Recent advances in novel nanostructuring methods of perovskite electrocatalysts for energy-related applications. Small Methods 2(7):1800071. https://doi.org/10.1002/smtd.201800071
6. Sun J, Zhang Z, Gong Y, Wang H, Wang R, Zhao L, He B (2019) Plasma engraved $Bi_{0.1}(Ba_{0.5}Sr_{0.5})_{0.9}Co_{0.8}Fe_{0.2}O_3-\delta$ perovskite for highly active and durable oxygen evolution. Sci Rep 9(1):4210. https://doi.org/10.1038/s41598-019-40972-1
7. Jiao Y, Zheng Y, Jaroniec M, Qiao SZ (2015) Design of electrocatalysts for oxygen- and hydrogen-involving energy conversion reactions. Chem Soc Rev 44(8):2060–2086. https://doi.org/10.1039/C4CS00470A
8. Lyu Y-Q, Ciucci F (2017) Activating the bifunctionality of a perovskite oxide toward oxygen reduction and oxygen evolution reactions. ACS Appl Mater Interfaces 9(41):35829–35836. https://doi.org/10.1021/acsami.7b10216
9. Suntivich J, May KJ, Gasteiger HA, Goodenough JB, Shao-Horn Y (2011) A perovskite oxide optimized for oxygen evolution catalysis from molecular orbital principles. Science 334(6061):1383. https://doi.org/10.1126/science.1212858
10. Zhao B, Zhang L, Zhen D, Yoo S, Ding Y, Chen D, Chen Y, Zhang Q, Doyle B, Xiong X, Liu M (2017) A tailored double perovskite nanofiber catalyst enables ultrafast oxygen evolution. Nat Commun 8(1):14586. https://doi.org/10.1038/ncomms14586
11. Zhu Y, Zhou W, Chen Z-G, Chen Y, Su C, Tadé MO, Shao Z (2015) $SrNb_{0.1}Co_{0.7}Fe_{0.2}O_3-\delta$ perovskite as a next-generation electrocatalyst for oxygen evolution in alkaline solution. Angew Chem Int Ed 54(13):3897–3901. https://doi.org/10.1002/anie.201408998
12. Jung J-I, Risch M, Park S, Kim MG, Nam G, Jeong H-Y, Shao-Horn Y, Cho J (2016) Optimizing nanoparticle perovskite for bifunctional oxygen electrocatalysis. Energy Environ Sci 9(1):176–183. https://doi.org/10.1039/C5EE03124A
13. May KJ, Carlton CE, Stoerzinger KA, Risch M, Suntivich J, Lee Y-L, Grimaud A, Shao-Horn Y (2012) Influence of oxygen evolution during water oxidation on the surface of perovskite oxide catalysts. J Phys Chem Lett 3(22):3264–3270. https://doi.org/10.1021/jz301414z
14. Xu X, Pan Y, Zhou W, Chen Y, Zhang Z, Shao Z (2016) Toward enhanced oxygen evolution on perovskite oxides synthesized from different approaches: a case study of $Ba_{0.5}Sr_{0.5}Co_{0.8}Fe_{0.2}O_3-\delta$. Electrochim Acta 219:553–559. https://doi.org/10.1016/j.electacta.2016.10.031
15. Li Z, Fu J-Y, Feng Y, Dong C-K, Liu H, Du X-W (2019) A silver catalyst activated by stacking faults for the hydrogen evolution reaction. Nat Catal 2(12):1107–1114. https://doi.org/10.1038/s41929-019-0365-9
16. Xia Y (2019) In my element: silver. Chem A Eur J 25(17):4244–4244. https://doi.org/10.1002/chem.201805675
17. Zhou Y, Lu Q, Zhuang Z, Hutchings GS, Kattel S, Yan Y, Chen JG, Xiao JQ, Jiao F (2015) Oxygen reduction at very low overpotential on nanoporous Ag catalysts. Adv Energy Mater 5(13):1500149. https://doi.org/10.1002/aenm.201500149
18. Liu R, Ye K, Gao Y, Zhang W, Wang G, Cao D (2015) Ag supported on carbon fiber cloth as the catalyst for hydrazine oxidation in alkaline medium. Electrochim Acta 186:239–244. https://doi.org/10.1016/j.electacta.2015.10.126
19. Zhuang S, Huang K, Huang C, Huang H, Liu S, Fan M (2011) Preparation of silver-modified $La_{0.6}Ca_{0.4}CoO_3$ binary electrocatalyst for bi-functional air electrodes in alkaline medium. J Power Sour 196(8):4019–4025. https://doi.org/10.1016/j.jpowsour.2010.11.056
20. Ananth MV, Manimaran K, Arul Raj I, Sureka N (2007) Influence of air electrode electrocatalysts on performance of air-MH cells. Int J Hydrogen Energy 32(17):4267–4271. https://doi.org/10.1016/j.ijhydene.2007.06.008
21. Wagner N, Schulze M, Gülzow E (2004) Long term investigations of silver cathodes for alkaline fuel cells. J Power Sources 127(1):264–272. https://doi.org/10.1016/j.jpowsour.2003.09.022
22. Zhang Y, Liu J, Huang X, Lu Z, Su W (2008) Low temperature solid oxide fuel cell with $Ba_{0.5}Sr_{0.5}Co_{0.8}Fe_{0.2}O_3$ cathode prepared by screen printing. Solid State Ionics 179(7):250–255. https://doi.org/10.1016/j.ssi.2008.02.008
23. Liang F, Zhou W, Li J, Zhu Z (2013) Microwave-plasma induced reconstruction of silver catalysts for highly efficient oxygen reduction. J Mater Chem A 1(44):13746–13749. https://doi.org/10.1039/C3TA13656F
24. Park CY, Lee TH, Dorris SE, Park JH, Balachandran U (2012) Ethanol reforming using $Ba_{0.5}Sr_{0.5}Cu_{0.2}Fe_{0.8}O_3-\delta$/Ag composites as oxygen transport membranes. J Power Sources 214:337–343. https://doi.org/10.1016/j.jpowsour.2012.04.052
25. quot, Chatrchyan S, quot, quot, Khachatryan V, quot, quot, Sirunyan AM, quot, quot, Collaboration: The CMS, Collaborations T, quot, quot, others a, quot Measurement of pseudorapidity distributions of charged particles in proton-proton collisions at $\sqrt{(s)} = 8$ TeV by the CMS and TOTEM experiments. https://doi.org/10.1140/EPJC/S10052-014-3053-6
26. Mosiałek M, Michna A, Dziubaniuk M, Bielańska E, Kežionis A, Šalkus T, Kazakevičius E, Bożek B, Krawczyk A, Wyrwa J, Orliukas AF (2018) Composite cathode material LSCF-Ag for solid oxide fuel cells obtained in one step sintering procedure. Electrochim Acta 282:427–436. https://doi.org/10.1016/j.electacta.2018.06.063
27. Zhu WX, Lü Z, Wang LX, Guan XY, Zhang XY (2011) Performance of $Ba_{0.5}Sr_{0.5}Co_{0.8}Fe_{0.2}O_3$-δ-Ag composite cathode materials for IT-SOFCs. Adv Mater Res 311–313:2309–2314. https://doi.org/10.4028/www.scientific.net/AMR.311-313.2309
28. Zhou W, Ran R, Shao Z, Cai R, Jin W, Xu N, Ahn J (2008) Electrochemical performance of silver-modified $Ba_{0.5}Sr_{0.5}Co_{0.8}Fe_{0.2}O_3-\delta$ cathodes prepared via electroless deposition. Electrochim Acta 53(13):4370–4380. https://doi.org/10.1016/j.electacta.2008.01.058
29. Leo A, Liu S, Diniz da Costa JC (2009) The enhancement of oxygen flux on $Ba_{0.5}Sr_{0.5}Co_{0.8}Fe_{0.2}O_3-\delta$ (BSCF) hollow fibers using silver surface modification. J Membr Sci 340(1):148–153. https://doi.org/10.1016/j.memsci.2009.05.022
30. Yusop UA, Huai TK, Rahman HA, Baharuddin NA, Raharjo J (2020) Electrochemical performance of barium strontium cobalt ferrite -samarium doped ceria- argentum for low temperature solid oxide fuel cell. Mater Sci Forum 991:94–100. https://doi.org/10.4028/www.scientific.net/MSF.991.94
31. Lin Y, Ran R, Shao Z (2010) Silver-modified $Ba_{0.5}Sr_{0.5}Co_{0.8}Fe_{0.2}O_3-\delta$ as cathodes for a proton conducting

solid-oxide fuel cell. Int J Hydrogen Energy 35(15):8281–8288. https://doi.org/10.1016/j.ijhydene.2009.12.017
32. Felix C, Bladergroen BJ, Linkov V, Pollet BG, Pasupathi S (2019) Ex-situ electrochemical characterization of IrO2 synthesized by a modified adams fusion method for the oxygen evolution reaction. Catalysts 9(4):318
33. McCrory CCL, Jung S, Peters JC, Jaramillo TF (2013) Benchmarking heterogeneous electrocatalysts for the oxygen evolution reaction. J Am Chem Soc 135(45):16977–16987. https://doi.org/10.1021/ja407115p
34. Wen Y, Zhang C, He H, Yu Y, Teraoka Y (2007) Catalytic oxidation of nitrogen monoxide over $La_{1-x}Ce_xCoO_3$ perovskites. Catal Today 126(3):400–405. https://doi.org/10.1016/j.cattod.2007.06.032
35. Fabbri E, Nachtegaal M, Binninger T, Cheng X, Kim B-J, Durst J, Bozza F, Graule T, Schäublin R, Wiles L, Pertoso M, Danilovic N, Ayers KE, Schmidt TJ (2017) Dynamic surface self-reconstruction is the key of highly active perovskite nano-electrocatalysts for water splitting. Nat Mater 16:925. https://doi.org/10.1038/nmat4938. https://www.nature.com/articles/nmat4938#supplementary-information
36. Norman C, Leach C (2011) In situ high temperature X-ray photoelectron spectroscopy study of barium strontium iron cobalt oxide. J Membr Sci 382(1):158–165. https://doi.org/10.1016/j.memsci.2011.08.006
37. Xu X, Chen Y, Zhou W, Zhu Z, Su C, Liu M, Shao Z (2016) A perovskite electrocatalyst for efficient hydrogen evolution reaction. Adv Mater 28(30):6442–6448. https://doi.org/10.1002/adma.201600005

Affiliations

Emre Yusuf Göl[1] · Ahmet Aytekin[1] · Ecem Ezgi Özkahraman[1] · Engin Karabudak[1]

✉ Engin Karabudak
enginkarabudak@iyte.edu.tr

[1] Department of Chemistry, Faculty of Science, İzmir Institute of Technology, Gülbahçe Campus, 35433 Urla, İzmir, Turkey